ARTICLE
Journal of Cellular Biochemistry 110:1175–1186 (2010)

Journal of Cellular Biochemistry

QSG-7701 Human Hepatocytes Form Polarized Acini in Three-Dimensional Culture

Fang Zhang,[1] Ren Xu,[2] and Mu-jun Zhao[1*]

[1] *State Key Laboratory of Molecular Biology, Institute of Biochemistry and Cell Biology, Shanghai Institutes for Biological Sciences, Chinese Academy of Sciences, Shanghai 200031, China*

[2] *Life Sciences Division, Lawrence Berkeley National Laboratory, Berkeley, California 94720*

ABSTRACT

Hepatocytes are polarized and fulfill a variety of liver-specific functions in vivo; but the polarized tissue structure and many of these functions are lost when the cells are cultured on plastic. To recapitulate the polarized structure and tissue-specific function of liver cells in culture, we established a three-dimensional (3D) culture assay with the human hepatocyte line QSG-7701. In 3D Matrigel culture, QSG-7701 cells formed polarized spheroids with a center lumen, which is reminiscent of bile canaliculi in the liver. Immunofluoresence analysis showed that F-actin bundles and radixin were mainly located at the apical membrane and that α6 and β1 integrins were localized basally in 3D culture. Lumen formation was associated with the selective apoptosis of centrally located cells and was accompanied by proliferative suppression during acinar development. Compared to QSG-7701 cells in 2D or agarose gel cultures, the cells in 3D Matrigel culture maintained a given direction of biliary excretion and acquired higher levels of cytochrome P450 and albumin expression. Our study shows that the immortal human hepatocytes, QSG-7701, in 3D Matrigel culture reacquire cardinal features of glandular epithelium in vivo, providing an ex vivo model to study liver-specific function and tumorigenesis. J. Cell. Biochem. 110: 1175–1186, 2010.

KEY WORDS: HEPATOCYTES; THREE-DIMENSIONAL CULTURE; MORPHOGENESIS; POLARITY; ACINUS; BILE CANALICULUS

Hepatocytes (liver parenchymal cells) are polarized in vivo and perform multiple functions critical to the well-being of an organism, including protein synthesis, metabolism, detoxification, and excretion. Hepatocytes possess a belt of apical (bile canalicular) surface of adjacent cells that form microvillus-lined lumens, and two basolateral (sinusoidal) surfaces, both of which are specialized for exchange of metabolites with the blood, extend into the space of Disse in vivo [Sasse et al., 1992]. The apical and basal surfaces have distinct protein composition and function. Ezrin-Radixin-Moesin (ERM) protein in hepatocytes mainly localizes at the apical bile canalicular membrane [Wang et al., 2006], while integrins are localized to the basolateral membranes mediating cell–extracellular matrix (ECM) interactions [O'Brien et al., 2002; Tanimizu et al., 2007]. Bile acid is excreted into the bile duct by traversing the apical surface, whereas albumin is secreted into the circulation from the basal surface [Sasse et al., 1992].

The dynamic reciprocal interactions between ECM and cells generate the physical and biochemical signals that play a crucial role in regulating tissue architecture and specificity [Nelson and Bissell, 2006; Xu et al., 2009]. When placed in standard monolayer cultures, hepatocytes rapidly dedifferentiate, changing their cuboidal and polarized morphology, and losing liver-specific functions in the absence of the proper ECM microenvironment [LeCluyse et al., 1996]. Over the past decade, several approaches to maintain the long-term differentiated phenotype in vitro have been described [Bissell et al., 1987; Dunn et al., 1991; LeCluyse et al., 1996]. One approach is culturing hepatocytes in 3D collagen gels, which allow hepatocytes to re-establish in vivo-like tissue structure and to maintain liver-specific functions at certain levels [Dunn et al., 1991; Richert et al., 2002]. Matrigel, a laminin-rich ECM derived from the Engelbreth-Holm-Swarm (EHS) mouse sarcoma, has been reported to provide a proper microenvironment for the hepatocyte

Abbreviations used: 3D, three-dimensional; ERM, Ezrin-Radixin-Moesin; ECM, extracellular matrix; EHS, Engelbreth-Holm-Swarm; MDCK cells, Madin-Darby Canine Kidney cells; DAPI, 4′,6-diamidino-2-phenylindole; FDA, fluorescein diacetate; PMS, phenazine methosulfate.

Grant sponsor: National Key Science & Technology Special Project of China; Grant numbers: 2008ZX10002-020, 2008ZX10002-017.

*Correspondence to: Prof. Mu-jun Zhao, Institute of Biochem & Cell Biology, SIBS, Chinese Academy of Sciences, 320 Yue Yang Road, Shanghai 200031, China. E-mail: mjzhao@sibs.ac.cn

Received 16 July 2009; Accepted 25 March 2010 • DOI 10.1002/jcb.22632 • © 2010 Wiley-Liss, Inc.
Published online 19 May 2010 in Wiley InterScience (www.interscience.wiley.com).

growth and differentiation [Stamatoglou and Hughes, 1994; Moghe et al., 1996; Haouzi et al., 2005].

Acini, also known as cysts in the salivary gland, alveoli in the lung, and follicles in the thyroid, are spherical mono- or dual-layers of cells that enclose a central lumen in vivo, which are structural and functional units in many internal epithelial organs. Unlike 2D cultures, the 3D culture provides a unique opportunity to model the architecture of epithelium in vitro. Mammary epithelial cells in 3D culture form growth-arrested polarized acini with a hollow lumen [Debnath et al., 2002], human salivary gland cells are capable of morphogenesis and differentiation to cysts in 3D culture [Joraku et al., 2007; Szlavik et al., 2008], thyroid cells organize into follicles [Toda and Sugihara, 1990; Yap et al., 1994], and Madin-Darby Canine Kidney (MDCK) cells form cysts and tubules [Pollack et al., 1998; Lin et al., 1999] in 3D cultures. Apoptosis has been shown to be critical for creating luminal space during acinar morphogenesis in MCF-10A mammary gland [Debnath et al., 2002] and HSG salivary gland 3D cultures [Szlavik et al., 2008]. The tight control of proliferation also plays an important role in acinar morphogenesis. It has been reported that over-expression of either the cyclin D1 or the E7 oncoprotein from the Human Papilloma Virus 16 results in delay in lumen clearance [Hebner et al., 2008]. Although highlighting morphological differences between the liver and other epithelial tissue, an acinar structure of hepatocytes has been described in vivo during organogenesis and regeneration [Stamatoglou and Hughes, 1994], and a central lumen structure has been detected in the regrouped small islands of primary rat hepatocytes in vitro [Landry et al., 1985]. In addition, small and large lumen structures, which recapitulate bile canaliculi in the liver, have been found in primary rat hepatocyte spheroids [Abu-Absi et al., 2002] and immortal murine hepatocyte spheroids in 3D culture [Haouzi et al., 2005].

Considering the diverse activities of the liver, it is not surprising that a large number of cell–ECM and cell–cell interactions are required for cytoarchitecture and tissue-specific functions of hepatocytes. Nevertheless, the fact is that hepatocytes grown in 2D culture differ considerably in their morphology, cell–cell and cell–matrix interactions from that of in 3D culture. Although a number of previous studies have described physiological 3D cultures for primary mouse hepatocytes and also for rat hepatocytes, very little is known about the features of normal human hepatocytes in 3D cultures. Here, we use an immortalized but non-transformed human hepatocyte cell line, QSG-7701 [Zhu, 1979] to evaluate its cytoarchitecture, proliferation, and hepato-specific functions in 3D Matrigel culture. We show that QSG-7701 cells form polarized acinar structure and acquire differentiated hepatocyte functions in 3D Matrigel cultures.

MATERIALS AND METHODS

REAGENTS AND CELL LINES

Matrigel™ Basement Membrane Matrix (Catalog No: 354234) was from BD Biosciences (Bedford, MA). Polyclonal rabbit anti-radixin antibody, TRITC-labeled phalloidin, 4′,6-diamidino-2-phenylindole (DAPI), XTT sodium salt, phenazine methosulfate (PMS), O^7-Ethylresorufin, and Fluorescein diacetate (FDA) were purchased from Sigma (St. Louis, MS). Polyclonal rabbit anti-caspase-3 antibody was from Cell Signaling Technology (Beverly, MA). Ki-67 monoclonal antibody was from Epitomics (Burlingame, CA). Monoclonal mouse anti-integrin α6 and anti-integrin β1 were kind gifts from Dr. Linghua Meng, Shanghai Institute of Materia Medica, Chinese Academy of Sciences (CAS), China. Monoclonal mouse anti-E-cadherin antibody was a gift from Prof. Xuejun Zhang and mouse anti-β-catenin was a gift from Prof. Lin Li, both of them from the Institute of Biochemistry and Cell Biology, CAS, China. FITC-conjugated anti-mouse, FITC-conjugated anti-rabbit, and TRITC-conjugated anti-mouse IgGs were from Jackson Laboratories (West Grove, PA). Cell culture medium RPMI-1640, fetal bovine serum (FBS), non-conjugated anti-mouse IgG, TRIzol reagent, and SuperScript II First-Strand Synthesis System were from Invitrogen (Carlsbad, CA). Low melting point Agarose II™ was from Amresco (Solon, OH). Human Albumin ELISA Quantitation Set was purchased from Bethyl Laboratories (Montgomery, TX). MOWIOL® 4-88 Reagent was from Calbiochem (La Jolla, CA). The human hepatocyte cell line QSG-7701 was obtained from the Cell Bank of the CAS (Shanghai, China).

CELL CULTURES

QSG-7701 cells were grown in RPMI-1640 medium supplemented with 10% (v/v) FBS containing 100 units/ml penicillin and 100 μg/ml kanamycin. The cells were cultured at 37°C in 5% CO_2. For 3D Matrigel cell cultures, gel substrates were first prepared by evenly distributing 80 μl/cm^2 Matrigel (10 mg/ml) onto a plastic surface and incubating them at 37°C for approximately 30 min. Monolayer grown cells were harvested by trypsinization, taken up in the complete medium and separated into single-cell suspension cells. About 1.5×10^4 cells were seeded onto the gelled Matrigel per cm^2 surface. Agitation of the plate in the x–y plane at intervals during incubation could assist with preventing cell concentration in the center of the well. The cells were then incubated at 37°C under 5% CO_2 for 30 min. After the cell adheres to the gel, 250 μl/cm^2 ice-chilled RPMI-1640 containing 4% FBS and 1 mg/ml Matrigel was added. The cells were grown at 37°C under 5% CO_2 for up to 1 week with medium change every day. For agarose gel cultures, 2.0×10^5 exponentially growing cells were suspended in 0.4 ml RPMI-1640 complete medium containing 0.35% low melting point agarose and overlaid on 0.5% agarose in 24-well plates. After gelling, the agarose gels were covered with RPMI-1640 complete medium.

LIGHT MICROSCOPY AND CONFOCAL MICROSCOPY

Cellular phase-contrast images and some fluorescence images were acquired using an Olympus IX51 inverted microscope with DP71 digital camera (Olympus, Japan). Confocal images were taken by a Leica TCS SP2 (Leica, Wetzlar, Germany) inverted laser-scanning confocal microscope equipped with an external argon laser. Images were captured using a HC PL APO CS 20.0 × 0.70 UV objective.

ANALYSIS OF CELLULAR PROLIFERATION

Proliferative status was determined by counting the number of cells per colony as well as XTT assay. Cell number per spheroid was determined by counting the number of DAPI stained nuclei per

organoid in cryosections of QSG-7701 cells in 3D. One hundred fifty organoids were counted for each time point. Cell proliferation and viability was quantified by measuring absorbance at 492 nm after exposure of cells to XTT, which becomes metabolized by mitochondrial dehydrogenase to yield a formazan dye. In brief, cells were transferred to 96-well plates at 2×10^3 cells/well and cultured for 1–7 days. Absorbance was measured after a further 4 h incubation at 37°C with a solution of XTT (0.33 mg/ml) that contained 0.2 mg/ml PMS. The spectrophotometric absorbance of the sample was measured using an ELX800 microtiter plate reader (Bio-Tek Instruments).

SAMPLE PREPARATION AND IMMUNOFLUORESCENCE

3D culture samples were washed several times with ice-cold PBS, smeared and fixed on slides in either 1:1 methanol–acetone at −20°C for 2–3 min or 4% paraformaldehyde at ambient temperature for 20 min. The fixed structures were permeabilized for 2–5 min in 0.2% Triton X-100, rinsed with PBS–glycine (130 mM NaCl, 13 mM Na_2HPO_4, 3.5 mM NaH_2PO_4, 100 mM glycine) three times for 20 min, and then blocked with IF buffer [130 mM NaCl, 13 mM Na_2HPO_4, 3.5 mM NaH_2PO_4, 0.05% (w/v) NaN_3, 0.1% (w/v) BSA, 0.2% (v/v) Trition, 0.05% (v/v) Tween-20] containing 10% (v/v) goat serum and 8 μg/ml non-conjugated anti-mouse IgG at room temperature for 1 h. Primary antibodies were diluted in the blocking buffer described above and incubated at room temperature for 2 h or at 4°C overnight. Unbound primary antibodies were removed by washing three times in IF buffer three times for 20 min. Secondary antibodies were diluted in IF buffer containing 10% goat serum and incubated for 45–60 min. Unbound secondary antibodies were washed as described above. Finally, samples were incubated for 30–40 min with PBS containing 1 μg/ml TRITC-labeled phalloidin and stained for 3–5 min with 0.5 μg/ml DAPI before being mounted with the anti-fade agent Mowiol.

BILIARY EXCRETION OF FLUORESCEIN DIACETATE

A stock solution of 1 mg/ml FDA acetone (stored at −20°C) was diluted to 0.05 mg/ml FDA by adding a sample of the stock directly to the medium of cells grown in tissue culture dishes [Rotman and Papermaster, 1966; Shanks et al., 1994]. After 35 min incubation at 37°C, the FDA solution was removed, and the cells were rinsed twice with PBS, changed medium and then incubated at 37°C for 10–15 min. The cells were rinsed and mounted with Mowiol, and analyzed with an Olympus IX51 plus digital camera DP71 fluorescence microscope within 15 min.

RT-PCR AND REAL-TIME PCR

Total RNA was extracted from cultured cells using TRIzol reagent. cDNA was synthesized from 500 ng RNA samples using oligo(dT)18 primer and SuperScript II First-Strand Synthesis System in a reaction volume of 20 μl according to the manufacturer's instructions. PCR amplifications were performed using specific primers (Table I) and Ex Taq polymerase (TaKaRa) in a final volume of 25 μl. Glyceraldehyde-3-phosphate dehydrogenase (GAPDH) was amplified and used as a loading control. The amplified PCR products were electrophoresed on a 2% agarose gel containing 0.5 μg/ml ethidium bromide for nucleic acid visualization under UV light. Quantitative real-time PCR analysis was performed with Rotor Gene 6000 (Corbett Research, Australia) using the SYBR Green PCR

TABLE I. Primer Sequences With Annealing Temperatures and Positive Control Used for Each Primer Set

Primer	Sequence	Product size (bp)	Annealing temperature (°C)	Positive control
GAPDH	S: 5′-AGAAGGCTGGGGCTCATTTG-3′ A: 5′-AGGGGCCATCCACAGTCTTC-3′	266	55	–
CYP1A1	S: 5′-TGATAAGCACGTTGCAGGAG-3′ A: 5′-CAGCTCCAAAGAGGTCCAAG-3′	444	57	–
CYP1B1	S:5′-TGATGGACGCCTTTATCCTC-3′ A:5′-TGGTAGCCCAAGACAGAGGT-3′	364	57	–
CYP2C9	S: 5′-CTGAAACCCATAGTGGTGCTG-3′ A: 5′-TGAAAGTGGGATCACAGGGTG-3′	295	55	–
CYP3A4	S:5′-CCAAGCTATGCTCTTCACCG-3′ A:5′-TCAGGCTCCACTTACGGTGC-3′	324	52	–
Notch 1	S:5′-CCGTCATCTCCGACTTCATCT-3′ A:5′-GTGTCTCCTCCCTGTTGTTCTG-3′	468	52	HUVECs [Flynn et al., 2004]
Notch 2	S: 5′-GCTGATGCTGCCAAGCGT-3′ A:5′-CCGGGGAAGACGATCCAT-3′	474	55	HUVECs [Flynn et al., 2004]
Notch 3	S:5′-CGAAACCGCTCTACAGACTTGGAT-3′ A:5′-TCCTTGCTATCCTGCATGTCCTTAT-3′	239	62	Jurkat cell line [Flynn et al., 2004]
Notch 4	S:5′-TGCTGCTATGTGTCTCAGTGGTCAG-3′ A:5′-TTGGAACAGAAGGAGGGAGGAC-3′	346	63	HUVECs [Flynn et al., 2004]
CK 8	S: 5′-TGAGGTCAAGGCACAGTACGAG-3′ A: 5′-AACTTGGCGTTGGCATCCTTA-3′	276	57	HeLa cell line [Moll et al., 1982]
CK 18	S: 5′-GGGTTGACCGTGGAGGTAGATG-3′ A: 5′-CTCCATCTGTAGGGCGTAGCG-3′	315	57	HeLa cell line [Moll et al., 1982]
CK 7	S: 5′-CGGCATCATCGCTGAGGTCAA-3′ A: 5′-GGCACGCTGGTTCTTGATGTTG-3′	217	58	HeLa cell line [Moll et al., 1982]
CK 19	S: 5′-AGATTCTTGGTGCCACCATTGAGAA-3′ A: 5′-CAGCGTACTGATTTCCTCCT-3′	257	55	HT-29 cell line [Moll et al., 1982]
Integrinβ4	S:5′-ACAGGAGGGGTTAAAGCTGC-3′ A:5′-GCAGCTTTAACCCCTCCTGT-3′	416	55	HT-29 cell line [Simon-Assmann et al., 1994]

HUVECs, human umbilical vein endothelial cells.

Master Mix (TOYOBO). It consisted of 12.5 μl of SYBR Green PCR Master Mix, 1 μl of 10 mM forward and reverse primers, 10.5 μl of water, and 1 μl of diluted template cDNA in a total volume of 25 μl. The cycle conditions were as follows: 95°C for 3 min followed by 40 cycles (95°C denaturation for 15 s, 58°C annealing for 30 s, 72°C elongation for 30 s). Amplification was followed by melting curve analysis to verify the presence of a single PCR product. The mRNA levels of target genes were normalized according to the GAPDH mRNA levels.

ALBUMIN SYNTHESIS AND SECRETION ANALYSIS

Albumin expression was determined by both mRNA and protein levels. Albumin mRNA expression was measured by real-time PCR. Preparation of mRNA and cDNA synthesis was carried out as the method described above. Real-time PCR was performed using two pairs of primers. The primer pair (ALB-F, 5′-TGTTGCATGA-GAAAACGCCA-3′; ALB-R, 5′-GTCGCCTGTTCACCAAGGAT-3′) was used for amplifying a fragment containing human albumin exon 12 [Aarskog and Vedeler, 2000]. The primer pair for amplifying a 266-bp GAPDH gene, which was used as an internal control, was described in Table I. The PCR reaction was carried out as the method described above. The relative expression of albumin mRNA is normalized against GAPDH. The secretion of albumin was analyzed from the QSG-7701 cultured media samples by Human Albumin ELISA Quantitation Set. The absorbance was measured at 492 nm with a Multiskan MK 3 microplate reader (Thermo). Results are expressed per microgram DNA, which was analyzed fluorometrically with Hoechst dye 33258 (Sigma) [Labarca and Paigen, 1980; Dunn et al., 1991].

NORMALIZED 7-ETHOXYRESORUFIN-*O*-DEETHYLATION ASSAY

Normalized 7-ethoxyresorufin-*O*-deethylation assay has been used to measure the demethylation activity of cytochrome P450 (CYP) 1A-associated monooxygenase enzymes [Burke et al., 1985]. The cultures were incubated with 39.2 mM 7-ethoxyresorufin in culture medium at 37°C for 4 h. The amount of resorufin converted by the enzymes was calculated by measuring the resorufin fluorescence in the incubation medium at 530 nm (excitation)/580 nm (emission) against resorufin standards using a Cary Eclipse fluorescence spectrophotometer (Varian, Australia). Functional data were normalized to 2×10^5 cells based on the number of seeded cells.

STATISTICAL ANALYSIS

All data were presented as means ± standard deviation ($x \pm SD$). Each assay was performed at least five times independently. Statistical significance was tested by one-way ANOVA followed by Bonferroni or Tamhane post hoc using SPSS software. The statistical significance was set at a P-value of <0.05.

RESULTS

QSG-7701 FORMS ACINAR-LIKE STRUCTURE IN 3D MATRIGEL CULTURE

QSG-7701 cell line is a spontaneously immortalized liver epithelial cell line, which was originally derived from the non-tumor liver tissue of a 35-year-old patient with liver cancer [Zhu, 1979]. QSG-7701 cells formed monolayers on tissue plastic, and proliferated until confluency (Fig. 1A). When the cells were embedded in the agarose gel, they proliferated slowly and formed multicellular

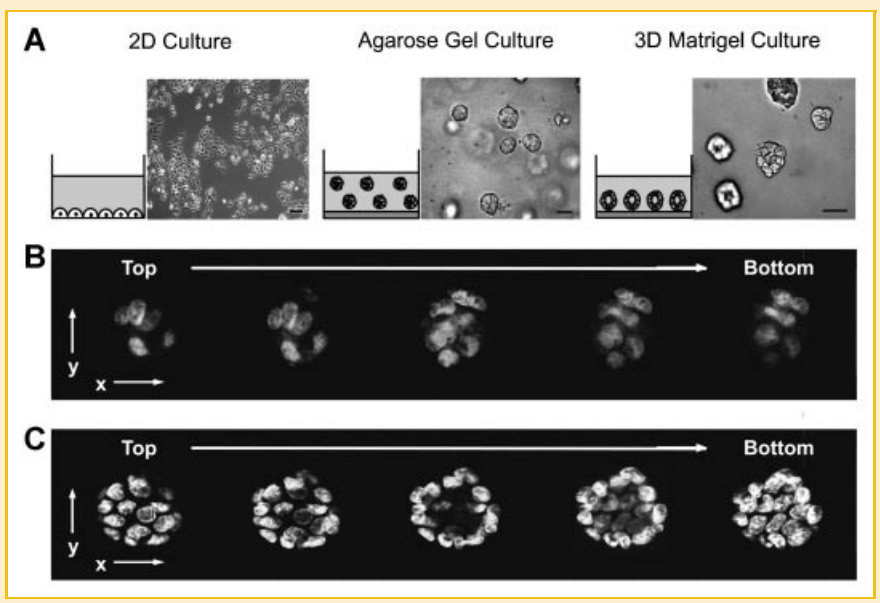

Fig. 1. Morphological changes of QSG-7701 cells in 2D, agarose gel and 3D Matrigel cultures. A: Schemes and phase-contrast images of QSG-7701 grown in 2D culture, agarose gel, and 3D Matrigel cultures. Scale bars, 50 μm. B: Representative serial confocal cross sections (x–y axis) through QSG-7701 spheroids cultured in agarose gel. C: Representative serial confocal cross sections (x–y axis) through QSG-7701 spheroids cultured in 3D Matrigel. [Color figure can be viewed in the online issue, which is available at www.interscience.wiley.com.]

spheroids (Fig. 1A). Confocal analysis of 160 structures showed that the spheroid in agarose gel did not contain lumen (Fig. 1B). However, when plated as single-cell suspensions on top of Matrigel, the cells proliferated and formed compact spheroids (Fig. 1A). We counted 530 structures from five independent experiments and found that 42.65% of the spheroids formed a hollow lumen at the center using confocal microscopy (Fig. 1C). These data suggest that QSG-7701 cells form acinar-like structures in 3D Matrigel culture which contained basal laminar components.

To determine how QSG-7701 cells develop into acinar-like spheroids, we monitored the spheroid morphogenesis with a phase contrast microscope. Cells adhered on Matrigel within 12 h, with most of them structurally round (Fig. 2a,a′). They kept proliferating (Fig. 2b,b′,c,c′) and formed larger compact spherical structures within the next five days (Fig. 2d,d′). Dense granules appeared in the bodies of the acinar-like structures whereas most cells in the interior of the spheroids started to die at day 5 (Fig. 2d, arrow). A hollow lumen was detectable in the center of the spheroid at day 7 (Fig. 2e,e′). Once the acinar structures were established, the average acinar size did not increase any more, suggesting that most cells were growth arrest (data not shown). A few larger structures were observed, which was most likely due to the heterogeneity of QSG-7701 cells.

QSG-7701 ESTABLISHES APICAL AND BASAL POLARITY IN 3D MATRIGEL CULTURE

Epithelial cell polarity is largely dependent on the proper cell-ECM and cell–cell interactions [Nelson and Bissell, 2006; Xu et al., 2009]. Establishment of hepatocyte polarity can be detected by certain apical and basal markers: cortically distributed F-actin and ERM have been used as apical canalicular membrane structure markers in hepatocytes [Haouzi et al., 2005; Wang et al., 2006], while intergin α6 and β1 are used as basal markers of epithelial cells [O'Brien et al., 2002; Tanimizu et al., 2007]. Therefore, we examined the cell apical polarity by detecting the organization of actin filaments (F-actin) in QSG-7701 spheroids at day 4 or 5 when 3D structures started to be formed. A total of 170 structures were analyzed and 45% of the spheroids were found Phalloidin–TRITC labeling of F-actin particularly intense around the lumen, which revealed a strong presence of microvillus-lined apical domains (Fig. 3A). We also analyzed distribution of radixin, a dominant ERM protein whose association with bile canalicular membranes is essential for normal liver function [Wang et al., 2006]. Radixin was detected at the surfaces bordering the lumens in 3D spheroids (Fig. 3A) indicating that QSG-7701 established apical polarity in 3D Matrigel culture at an early stage of acinar morphogenesis. To determine whether QSG-7701 spheroids in 3D Matrigel culture establish basal polarity, we performed immunofluorescence analysis with an antibody against β1 integrin. A total of 100 spheroids were counted and 51% structures were stained with β1 integrin, whose localization was specific to the basal membrane (Fig. 3B). Likewise, we did analysis with an antibody against α6 integrin. Images showed that α6 integrin also localized at the basal membrane (Fig. 3B). Both β1 and α6 integrins were stained at the basal membrane indicated that QSG-7701 spheroids in 3D Matrigel culture established basal polarity. We also detected the localization of E-cadherin and β-catenin in 3D spheroids by immunofluorescence. The results showed that E-cadherin and β-catenin were mainly laterally localized (Fig. 3C), indicating cell–cell junctions of the spheroids in 3D Matrigel. We counted 200 structures immunostained with antibody against β-catenin and found 43% of them were positive for this marker. Taken together, these data indicate that QSG-7701 cells could form polarized acini in 3D Matrigel culture.

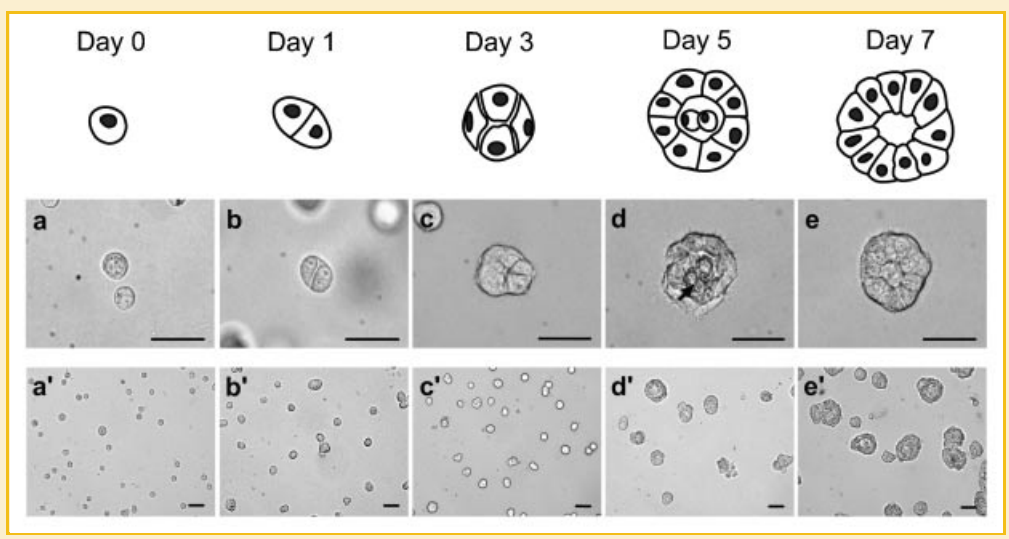

Fig. 2. Acinar morphogenesis of QSG-7701 in 3D Matrigel culture. Schemes of QSG-7701 cells grown in 3D Matrigel from days 0 to 7 are illustrated on the top. Corresponding phase-contrast images are shown at different magnification in the lower part of the schemes. Single-suspended cells were incubated at day 0 in 3D (a). The cells continued to proliferate for several days, forming compact spheroids filled with cells (b–c), whereas most cells in the interior of the spheroids (arrow) started to die at day 5 (d). After 7 days, acini with a hollow lumen (e) were formed. Scale bars, 50 μm. [Color figure can be viewed in the online issue, which is available at www.interscience.wiley.com.]

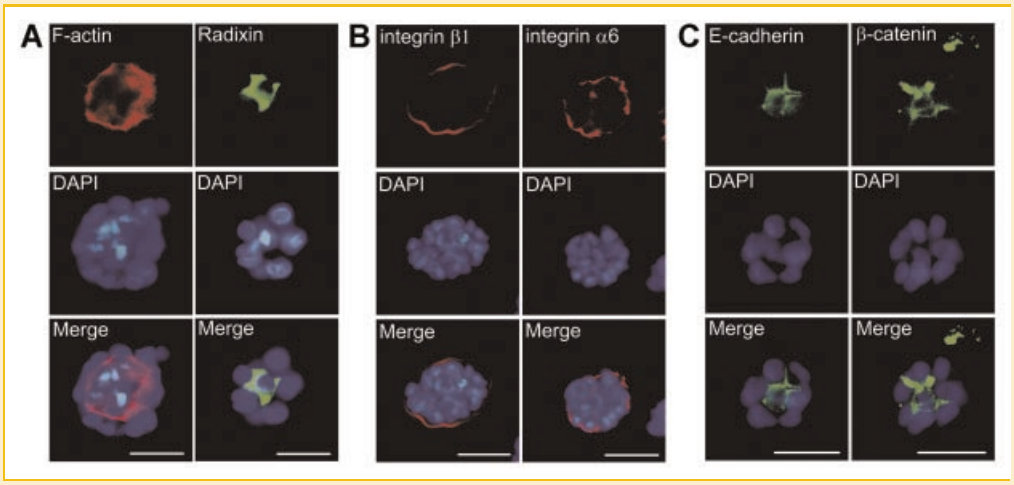

Fig. 3. Apical and basal polarity of QSG-7701 cells in 3D Matrigel culture. A: The apical polarity of QSG-7701 cells in 3D was detected by cortically distributed F-actin and radixin. Both F-actin (Phalloidin-TRITC, red) and radixin (FITC, green) decorate the lumen-exposed membranes of spheroids. Nuclei are stained with DAPI (blue). B: The basal polarity of QSG-7701 spheroids is examined by β1 and α6-integrins. Both β1- and α6-integrins (TRITC, red) are targeted to the basal membrane. All the cells were analyzed 4 days after cultured in 3D. C: Immunofluorescence microscopy images of E-cadherin (FITC, green) and β-catenin (FITC, green). Both of them are localized at the cell–cell junctions of the spheroids. Scale bars, 25 μm. [Color figure can be viewed in the online issue, which is available at www.interscience.wiley.com.]

PROLIFERATION AND APOPTOSIS OF QSG-7701 IN 3D MATRIGEL CULTURE

Acinar morphogenesis in 3D culture is usually accompanied by a decrease of cell proliferation and programmed cell death [Debnath et al., 2002; O'Brien et al., 2002; Haouzi et al., 2005]. We characterized the proliferation of QSG-7701 cells in 3D Matrigel and 2D culture by XTT assay. From days 1 to 5, cells proliferated rapidly in both 2D and 3D Matrigel cultures, though slightly slower in 3D. At day 6, however, QSG-7701 cells in 3D stopped considerable increase ($P > 0.05$), whereas cells in 2D continued growing noticeably ($P < 0.001$). At day 7, the proliferation of cells in 3D had a slightly decline compared to that at day 6 ($P > 0.05$), whereas cells in 2D still kept growing ($P < 0.01$; Fig. 4A). These results showed that in 3D Matrigel culture QSG-7701 cells entered a plateau state after day 5, which is very different from cells in 2D. By counting the nucleus number after DAPI staining, we showed that QSG-7701 cell number per spheroid in 3D Matrigel increased significantly during the first 5 days and ceased growing after day 6 ($P > 0.05$; Fig. 4B). These results indicated that the total cell numbers in 3D Matrigel do not increase after day 6, suggesting that the acini had reached a "growth-arrested" state.

We also investigated the correlation between cell proliferation and the acinar morphogenesis by immunostaining with an antibody against Ki-67, a nuclear protein that is only expressed during late G1 through M phase [Scholzen and Gerdes, 2000] and by measuring the diameters of acini. The immunostained images showed that the cell proliferation in 3D was active during the early stage of acinar morphogenesis, and a dramatic decline of Ki-67 positive cells was observed at day 7 (Fig. 4C). We counted at least 150 spheroids for each time point and found that 80%, 83%, 42%, and 11% of the QSG-7701 spheroids in 3D were Ki-67 positive at days 1, 3, 5, and 7 respectively. Measuring the max diameter of spheroids during acinar formation, we found that the acinar size increased from 26.96 ± 3.35 μm at day 3, to 40.24 ± 6.05 μm at day 5, and reached a peak 44.2 ± 8.4 μm at day 7 (Fig. 4D). Together these results showed that the enlargement of acinar diameter associates with positive Ki-67 staining on cells and the cessation of the growth correlates with the reduction of proliferation, indicating that the acinar structures form through proliferation, but not by aggregation.

Activation of caspase-3 is a hallmark of programmed cell death. To characterize the apoptosis of QSG-7701 cells in 3D Matrigel, we detected the activated caspase-3 at day 4 or 5 by immunofluorescence analysis. The results showed that caspase-3 was activated in cells located inside the spheroid, and chromatin in those cells was condensed (Fig. 4E). The presence of apoptotic bodies inside the lumen indicated that apoptosis was implemented to form the acinar phenotype with luminal space. Taken together, proliferative suppression and apoptosis take part in acinar morphogenesis.

QSG-7701 ACQUIRES LIVER-SPECIFIC FUNCTION IN 3D MATRIGEL CULTURE

One characterization of polarized hepatocytes in vivo is that it can secret bile acid to bile canaliculi [Sasse et al., 1992]. To ascertain whether QSG-7701 grown in 3D retained functional characteristics of polarized hepatocytes, we first investigated the ability of hepatocytes to transport bile acids into the channels by a fluorescein diacetate (FDA) assay. FDA can assess the cellular ability of converting the non-fluorescent FDA into the green fluorescent compound "fluorescein" and transporting it into bile canaliculi [Rotman and Papermaster, 1966; Shanks et al., 1994]. In 2D culture, non-fluorescent FDA was taken up by cells and transformed into fluorescein, but the fluorescein was not able to be excreted efficiently or at all, causing intracellular accumulation (Fig. 5a′). Similar results were observed in agarose gel culture, which does not contain any basement membrane protein (Fig. 5b′). However, in contrast to cells in 2D or agarose gel culture, the spheroids in 3D Matrigel not only absorbed FDA from the basement membrane, but also excluded the fluorescein from the cells. Fluorescein either

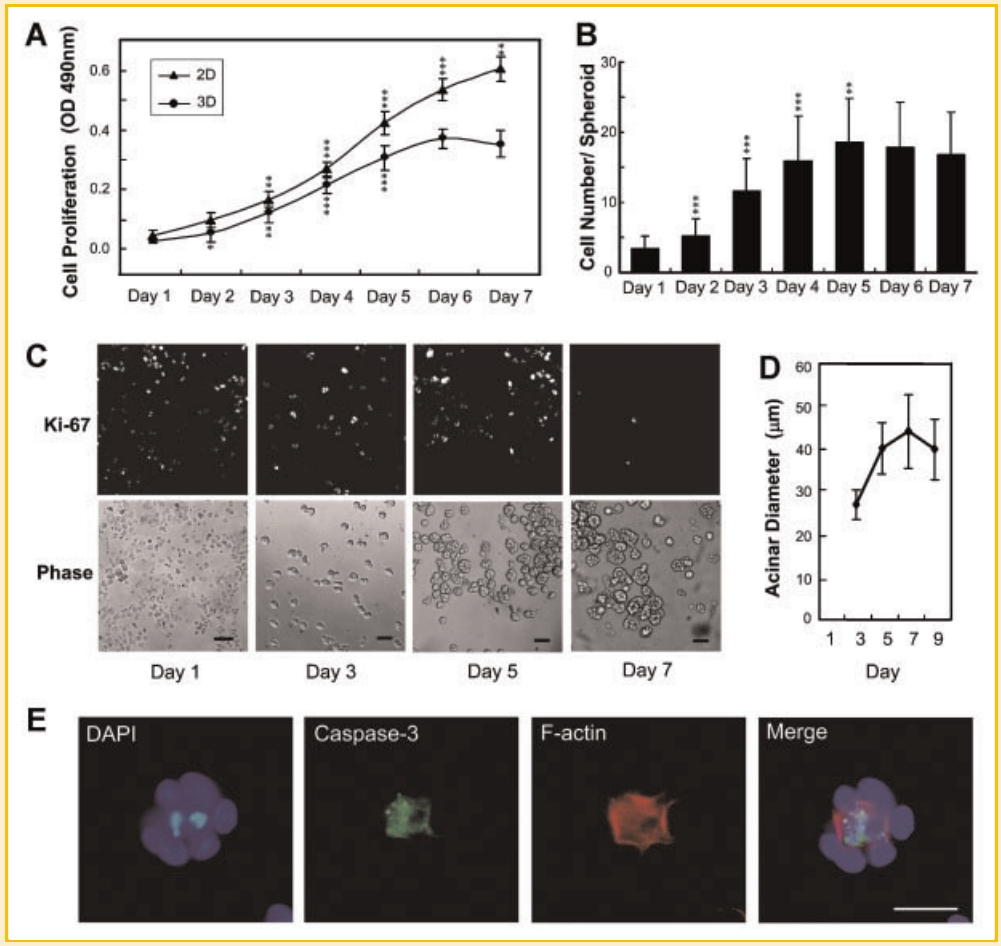

Fig. 4. Cell proliferation and apoptosis of QSG-7701 cells in 3D Matrigel culture. A: Cell proliferation of QSG-7701 in either 2D or 3D Matrigel culture was measured by XTT assay. Results are presented as the means ± SD of five to six independent experiments. The effect of incubation time on cell proliferation was assessed by comparing the present day cells to those of the day before the present. Effect of the incubation time was significant ($^{*}P < 0.05$, $^{**}P < 0.01$, $^{***}P < 0.001$). B: Proliferation status of QSG-7701 in 3D was determined by counting the number of cells per spheroid at different time points. The data are presented as the means ± SD of 150 colonies for each time point from five independent experiments. C: Cells grown in 3D for the indicated number of days, fixed, and immunostained with antibody against Ki-67. The corresponding phase-contrast images are shown in the lower column. Representative images show a dramatic decreasing numbers of Ki-67 positive cells within acini at day 7. Scale bars, 25 μm. D: The mean ± SD diameters of QSG-7701 acini after the indicated days in 3D are shown. For each time point, the diameters through the largest cross-section of 150–200 structures were measured. E: Cells were stained with DAPI after plated in 3D for 4–5 days. The cells in the interior, but not those of the exterior layer, contained fragmented nuclei (DAPI, blue) and were positively stained with anti-caspase-3 (FITC, green). F-actin (phalloidin-TRITC, red) was stained around the lumen. Scale bars, 25 μm. [Color figure can be viewed in the online issue, which is available at www.interscience.wiley.com.]

accumulated around the apical surface of the 3D spheroid (Fig. 5c′) or was secreted into the lumen (Fig. 5d′,e′), suggesting that bile acid flows in a given direction that reflects hepatic polarity in vivo. In summary, our results show that Matrigel which contained basal laminar components promotes human QSG-7701 hepatic cell line recapitulate bile canaliculi structure and excrete bile acid into the bile canaliculi in a functional way.

It has been shown that ECM signaling and polarized structure is critical for the activation and maintenance of liver-specific functions such as albumin secretion, and cytochrome P450 activities of hepatocytes [Ng et al., 2006]. We compared the albumin mRNA expression in QSG-7701 cells that cultured in 2D, agarose gel, and 3D Matrigel at day 5 by real-time PCR. The results showed that the levels of albumin mRNA were 3.5 times in agarose gel cells or 12.8 times in 3D Matrigel cells compared to that in 2D (Fig. 5B). We also examined the albumin secretion of cells in these culture conditions at day 5 by Human Albumin ELISA Quantitation Set. The rates of albumin secretion were 0.155, 0.161, and 0.215 μg/24 h/μg DNA in 2D, agarose gel, and 3D Matrigel cultures respectively (Fig. 5C). As a whole, these results indicate that 3D Matrigel, which is rich in basement membrane components enhances albumin expression and secretion of QSG-7701.

To investigate enzymatic detoxification and metabolic activities of hepatocyte in 3D, we compared cytochrome P450 activity in 2D, agarose gel, and 3D Matrigel cultured QSG-7701 cells at day 5 by the 7-ethoxyresorufin-*O*-deethylation (EROD) assay. The results showed that cytochrome P450 activities in agarose gel or 3D Matrigel were 2.9, or 6.2 times compared to that in 2D (Fig. 5D), indicating that P450 activity was increased in 3D Matrigel culture. Furthermore, we examined the expression of liver-specific CYP1, CYP2 and CYP3, the

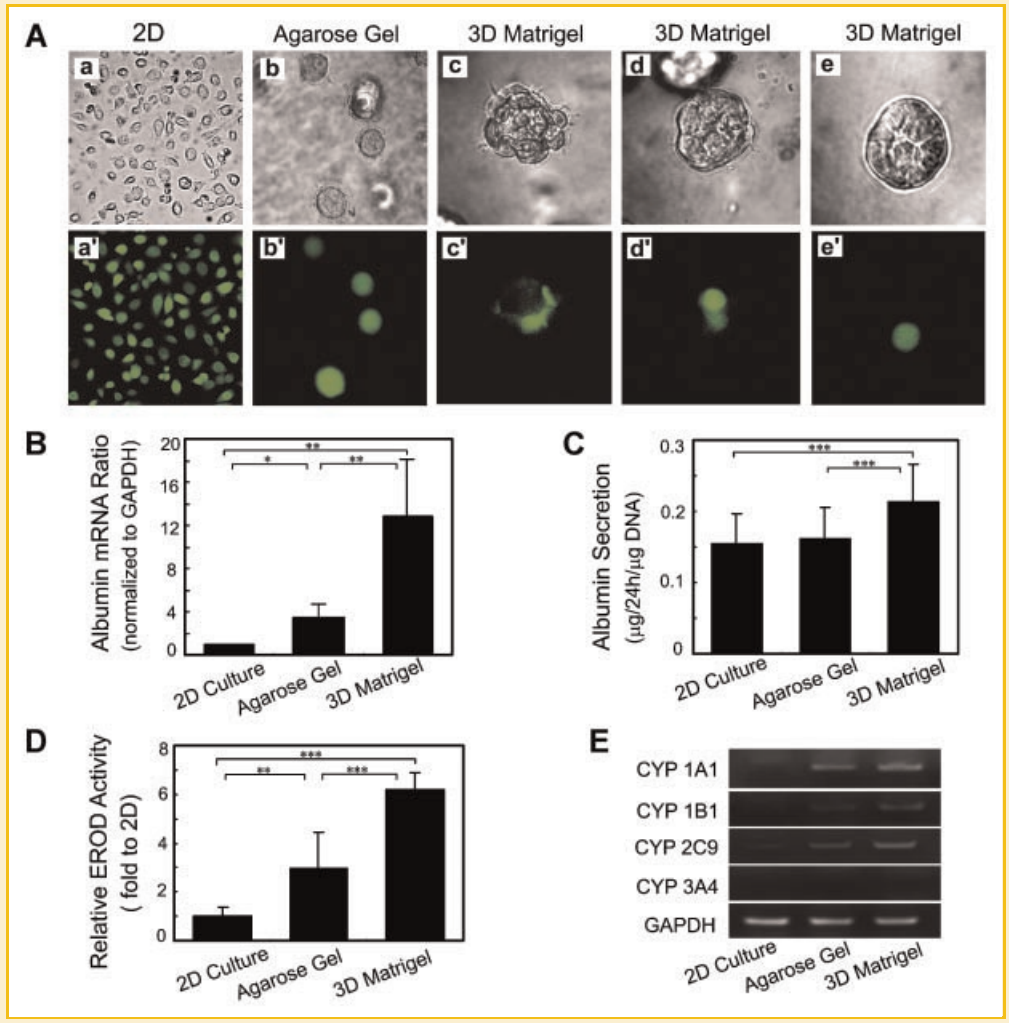

Fig. 5. Comparison of liver-specific functions of QSG-7701 cultured in 2D, agarose gel, and 3D Matrigel cultures. A: Bile canalicular secretion of FDA in QSG-7701 cells in 2D, agarose gel, and 3D Matrigel cultures. Cells were incubated with FDA for 35 min, and then incubated with fresh medium for 10–15 min. Secretion with fluorescein is remained in cells in 2D culture (a′), and the same results of cells in agarose gel culture (b′), whereas fluorescein is excreted into lumens in 3D Matrigel culture (c′,d′). B: Synthesis of albumin in QSG-7701 cells cultured in 2D, agarose gel, and 3D Matrigel cultures. Cells were cultured and harvested at day 5. mRNA levels of albumin were measured by real-time PCR and normalized to GAPDH. Results are expressed as the ratio between relative values of albumin mRNA in cells in agarose gel or 3D Matrigel to that in cells in 2D culture. C: Albumin secretion by QSG-7701 cells cultured in 2D, agarose gel, and 3D Matrigel cultures at day 5. The quantity of albumin secretion was measured by Human Albumin ELISA Quantitation Set. The results were normalized by the total DNA content. D: EROD cytochrome P450 activities of QSG-7701 cells in 2D, agarose gel, and 3D Matrigel cultures at day 5. The EROD activities of cells are fold to that in 2D. E: Expression of cytochrome P450 genes in QSG-7701 cultured in 2D, agarose gel, and 3D Matrigel cultures measured by RT-PCR. GAPDH expression was examined as an internal control. All data are represented as the means ± SD of five independent experiments. $^{*}P < 0.05$, $^{**}P < 0.01$, $^{***}P < 0.001$. [Color figure can be viewed in the online issue, which is available at www.interscience.wiley.com.]

members of human cytochrome P450 (CYP) subfamily, in 2D, agarose gel or 3D Matrigel cultured cells at day 5 by RT-PCR (Fig. 5E). Specific bands of CYP1A1 and 1B1 which are CYP1 subfamily genes were clearly detected in 3D Matrigel culture, whereas CYP1A1 RNA was expressed in agarose gel and barely detectable in 2D; CYP1B1 RNA expression was hardly detectable either in 2D or agarose gel culture. The expression of CYP2C9, a member of CYP2 subfamily, was similar to CYP1A1. The expression of CYP3A4 that belongs to CYP3 subfamily was no detectable either in all culture condition. GAPDH expression was examined as an internal control in this experiment. Together these results suggest that ECM signaling in 3D Matrigel is crucial for cytochrome P450 activation.

QSG-7701 ACINAR MORPHOGENESIS IS ACCOMPANIED WITH ACTIVATION OF NOTCH 4

It has been shown that Notch plays important roles in differentiation and tubule formation at distinct stages of development [Tanimizu and Miyajima, 2004; Ader et al., 2006; Zong et al., 2009]. In our study, we investigated whether Notch signaling take part in the lumen formation. We identified the expression of Notch family by RT-PCR. The results indicated that Notch 1 was not observed in QSG-7701cells cultured in 2D, agarose gel or 3D Matrigel during ainar formation. In contrast, Notch 2 was expressed at all cultured stages in 2D, agarose gel or 3D Matrigel. Interestingly, Notch 3 was not monitored in 2D or agarose gel, but a weak band in 3D Matrigel at day 7; only Notch 4 was strongly induced by 3D Matrigel, but not

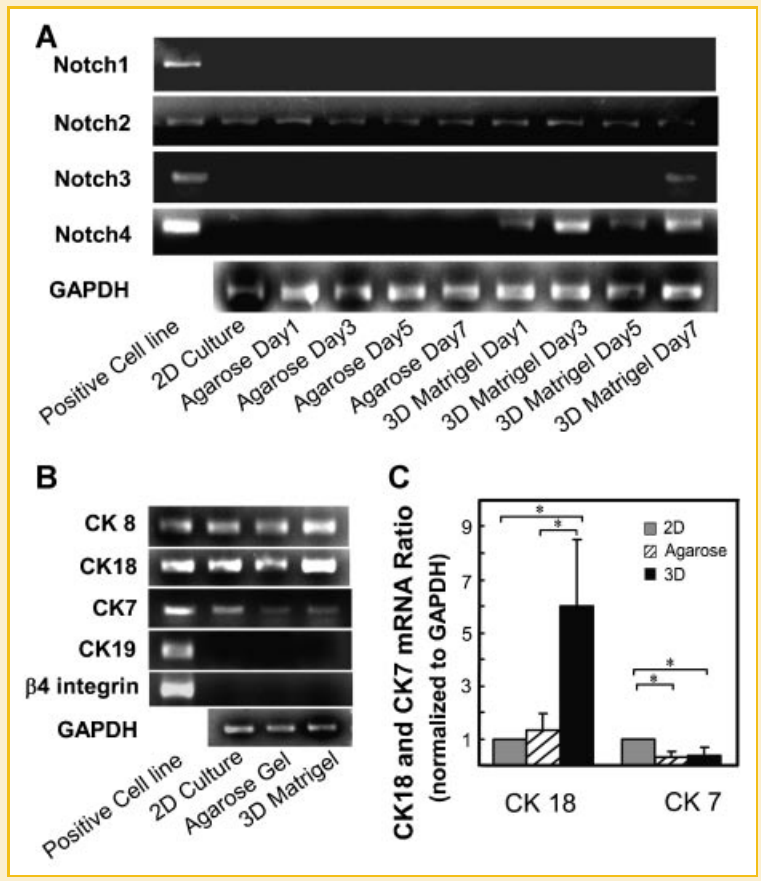

Fig. 6. The expression of Notch genes and phenotypic markers in QSG-7701 cells during acini formation. A: The expression of Notch 1–4 were monitored in cells in 2D, agarose gel, and 3D Matrigel cultures in different days by RT-PCR. GAPDH expression was examined as an internal control. Positive cell lines are given in Table I. B: The expression of hepatocyte markers (CK8 and CK18) and cholangiocyte markers (CK7, CK19) and integrin β4 of cells in 2D, agarose gel, and 3D Matrigel cultures were measured by RT-PCR. GAPDH expression was examined as an internal control. Positive cell lines are given in Table I. C: Real-time PCR analysis of the expression of CK18 and CK7 mRNA values in 2D, agarose gel, and 3D Matrigel cells. The mRNA levels of target genes were normalized to GAPDH. Results are expressed as the ratio between relative values of target mRNA in agarose gel or 3D Matrigel cells to that in 2D cells. All data represent the means ± SD of five independent experiments. $^{*}P < 0.05$.

detectable in 2D and agarose gel cultures (Fig. 6A). These results indicated that Notch 4 signaling was activated during lumen formation, and Notch 3 appeared to be activated at late stages of forming lumen.

Notch signaling controls liver development by coordinating biliary differentiation and morphogenesis [Zong et al., 2009]. Moreover, recent studies have demonstrated that mature rat hepatocytes can transdifferentiate into biliary epithelium both in vivo and in vitro [Nishikawa et al., 2005]. Thus, we wondered if QSG-7701 cells had transdifferentiated into bile duct cells as they formed acini in 3D Matrigel cultures. In our study, we found that QSG-7701 cells expressed cytokeratin 8 (CK8) and cytokeratin 18 (CK18), the phenotypic markers of hepatocytes [Moll et al., 1982], in all three cultures, weakly in 2D and agarose gel cultures, strongly in 3D Matrigel (Fig. 6B). We measured the CK18 mRNA levels in QSG-7701 cells at three different culture conditions by real-time PCR. The results showed that the levels of CK18 mRNA were 6.03 times in cells cultured in 3D compared to the cells in 2D (Fig. 6C). Culturing cells in agarose gel did not enhance CK18 expression significantly, suggesting ECM signaling is crucial for the hepatic differentiation in QSG-7701 cells. We further investigated the expression of phenotypic markers of cholangiocyte including cytokeratin 7 (CK7), cytokeratin 19 (CK19), and integrin β4 [Tanimizu et al., 2007]. We found that the cells expressed CK7, but not CK19 and integrin β4 in all three culture conditions (Fig. 6B). However, the levels of CK7 mRNA were much lower in the cells in agarose gel and 3D Matrigel compared to the cells in 2D cells (Fig. 6C). These results suggest that Matrigel did not induce cholangiocyte differentiation of QSG-7701.

DISCUSSION

QSG-7701 presents ill-differentiated phenotypic morphology and weak hepatic function in monolayer cultures [Zhu, 1979]. In our study, we showed that QSG-7701 cells in 3D Matrigel culture, form polarized acinar structure and reacquire liver-specific functions. The role of ECM in the control of development and differentiation has been intensely researched for many years. In several culture systems, the addition of ECM induces both cellular polarization and tissue

organization [Haouzi et al., 2005; Joraku et al., 2007; Szlavik et al., 2008; Xu et al., 2009]. The subendothelial space of hepatocytes in liver contains constituent proteins of a basal lamina, which affects hepatocelluar morphology and function [Bissell et al., 1987; Bissell and Choun, 1988].To better control the differentiation and cellular architecture of hepatocytes in vitro, the use of various components of the ECM has been explored in rodent hepatocyte culture [Moghe et al., 1996; Haouzi et al., 2005], and human primary cell culture [Kono et al., 1995]. In 1987, Dr. Montgomery Bissell showed that rat hepatocytes cultured on matrix components (laminin, type IV collagen, and heparin sulfate proteoglycan) have better ultrastructural morphology and hepatic function than on the individual basement membrane constituents [Bissell et al., 1987]. It shows that full support of hepatocelluar function requires a complex of ECM proteins. It is noteworthy that the molecular composition of Matrigel [Kleinman and Martin, 2005], a basement membrane matrix derived from the EHS mouse sarcoma, is similar to the basal lamina in the space of Disse in liver and provides a proper microenvironment to support hepatocyte growth and differentiation [Stamatoglou and Hughes, 1994; Moghe et al., 1996; Kleinman and Martin, 2005]. In addition to the use of various constituents of the ECM, altering the geometry of the ECM has been made to induce the formation of hepatocytes rather specialized polarity. It has been described that hepatocytes maintain long-term viability and function by sandwiching cells between two layers of ECM gel [Kono et al., 1995; Moghe et al., 1996; Haouzi et al., 2005]. Some studies report that using sandwich culture with an overlay of Matrigel gives a proper culture condition for hepatocytes instead of sandwich–collagen culture or a single layer of Matrigel [Haouzi et al., 2005; Schug et al., 2008]. We cultured QSG-7701 in 2D, agarose gel that does not have ECM components, and 3D Matrigel culture, respectively. The results show that only 3D Matrigel culture that contains basement membrane proteins can both upregulate liver-specific genes expression and induce cell polarization in hepatocytes, suggesting the crucial role of ECM in the control of liver development and differentiation.

In 3D Matrigel culture, QSG-7701 cells proliferated and organized into a polarized spheroid with a center lumen. Although the acini morphologies are found in several other epithelia in 3D systems [Pollack et al., 1998; Debnath et al., 2002; Szlavik et al., 2008] and some rodent hepatocytes [Bissell et al., 1987; Dunn et al., 1991; Haouzi et al., 2005], it seldom happens in human hepacotyes. It has been reported that a series of adjacent small lumens are formed in primary rat hepatocytes in 3D culture [Bissell et al., 1987; Dunn et al., 1991; Abu-Absi et al., 2002], and relative large lumens with small ones are also detected in the immortal murine mhAT3F hepatocytes [Haouzi et al., 2005]. A possible explanation for the structural heterogeneity of human and rodent hepatocytes in 3D culture might be the diversity in cell-intrinsic differentiation of species of hepatocytes. Moreover, the chemical composition of 3D matrix is also critical for the cytoarchitecture. For example, primary rat hepatocytes in the endogenous matrix deposited by aggregates of primary liver cells form acinar structure with a central lumen [Landry et al., 1985], whereas primary rat hepatocytes in collagen sandwich culture systems do not form those acinar structures [Moghe et al., 1996]. This might be one of the reasons why QSG-7701 form acini in 3D Matrigel but solid spheroids in agarose gel.

Notch plays important roles in differentiation and tubule formation at distinct stages of liver development. Notch could play a role in liver development by regulating a hepatocyte versus biliary epithelial cell fate choice and several studies have implicated that Notch is involved in the regulation of hepatoblast differentiation [Tanimizu and Miyajima, 2004; Ader et al., 2006]. In vitro experiments with mouse hepatoblasts were the first to suggest that the Notch pathway promotes biliary differentiation while silencing Notch 2 leads to hepatocyte differentiation [Tanimizu and Miyajima, 2004]. Moreover, recent studies have demonstrated that mature rat hepatocytes can transdifferentiate into biliary epithelium both in vivo and in vitro [Nishikawa et al., 2005]. In our study, we found that Notch 2 in QSG-7701 hepatocytes was expressed at all cultured stages in 2D, agarose gel or 3D Matrigel (Fig. 6A), implying that Notch 2 is not affected by hepatocyte differentiation or Matrigel induced lumen formation in QSG-7701 cells. We further identified hepatic characteristics of QSG-7701 cells. The results indicated that QSG-7701 cells expressed phenotypic markers of hepatocyte, such as CK8 and CK18, but did not express cholangiocyte markers, such as CK19 and integrin β4. Thus, we believe that QSG-7701 expressing Notch 2 is not due to transdifferentiation of hepatocytes into cholangiocytes. Interestingly, our results first indicated that basement membrane proteins could activate Notch 4 signaling in QSG-7701 cells during lumen formation. Therefore, Notch 4 might be very important for polarization of hepatocytes. Previous studies also revealed that the signals transduced through the Notch receptors, in combination with other cellular factors, directly regulate the expression of genes that influence proliferation, differentiation, and apoptosis events at all stages of development [Artavanis-Tsakonas et al., 1999]. Hence, whether the morphogenic changes depend upon activation of Notch 4 and how Notch 4 signaling affects lumen formation need to be further investigated.

Cell apoptosis occurred in the interior of the spheroid accompanying with proliferative suppression. It occurs in the lumen of 3D cultures of salivary gland [Szlavik et al., 2008], kidney[Pollack et al., 1998], and mammary epithelium [Debnath et al., 2002; Hebner et al., 2008], which is believed to reflect the physiological death during development in these organs. In our study, apoptosis clearly contributes to the lumen formation in QSG-7701 spheroids. In addition, the presence of apoptotic bodies are detected in some large lumens in the immortal murine hepatocytes in 3D culture [Haouzi et al., 2005]. Lumen can also be created without apoptosis. For example, separation of opposing membranes results in the generation of small lumens during thyroid cyst development in 3D culture [Yap et al., 1994], which may explain the formation of small lumens in some primary hepatocyte aggregations. We showed here that the large lumen structure is the bile canaliculus with bile excretion experiment, even though hepatocytes usually form small bile canaliculi in the liver. This might be a geometrical difference in vivo and in 3D cell culture that account for the altered phenotype of bile canaliculi. Overall, these results point to the utility of three-dimensional culture systems in modeling the liver tissue architecture and functions.

ACKNOWLEDGMENTS

We thank Dr. Linghua Meng of Shanghai Institute of Materia Medica, CAS, Prof. Xuejun Zhang and Prof. Lin Li from the Institute of Biochemistry and Cell Biology, CAS for kindly providing antibodies. This work was supported by the grants from the National Key S&T Special Project of China (No.2008ZX10002-020 and No.2008ZX10002-017).

REFERENCES

Aarskog NK, Vedeler CA. 2000. Real-time quantitative polymerase chain reaction. A new method that detects both the peripheral myelin protein 22 duplication in Charcot-Marie-Tooth type 1A disease and the peripheral myelin protein 22 deletion in hereditary neuropathy with liability to pressure palsies. Hum Genet 107:494–498.

Abu-Absi SF, Friend JR, Hansen LK, Hu WS. 2002. Structural polarity and functional bile canaliculi in rat hepatocyte spheroids. Exp Cell Res 274: 56–67.

Ader T, Norel R, Levoci L, Rogler LE. 2006. Transcriptional profiling implicates TGFbeta/BMP and Notch signaling pathways in ductular differentiation of fetal murine hepatoblasts. Mech Dev 123:177–194.

Artavanis-Tsakonas S, Rand MD, Lake RJ. 1999. Notch signaling: Cell fate control and signal integration in development. Science 284:770–776.

Bissell DM, Choun MO. 1988. The role of extracellular matrix in normal liver. Scand J Gastroenterol 151(Suppl):1–7.

Bissell DM, Arenson DM, Maher JJ, Roll FJ. 1987. Support of cultured hepatocytes by a laminin-rich gel. Evidence for a functionally significant subendothelial matrix in normal rat liver. J Clin Invest 79:801–812.

Burke MD, Thompson S, Elcombe CR, Halpert J, Haaparanta T, Mayer RT. 1985. Ethoxy-, pentoxy- and benzyloxyphenoxazones and homologues: A series of substrates to distinguish between different induced cytochromes P-450. Biochem Pharmacol 34:3337–3345.

Debnath J, Mills KR, Collins NL, Reginato MJ, Muthuswamy SK, Brugge JS. 2002. The role of apoptosis in creating and maintaining luminal space within normal and oncogene-expressing mammary acini. Cell 111: 29–40.

Dunn JC, Tompkins RG, Yarmush ML. 1991. Long-term in vitro function of adult hepatocytes in a collagen sandwich configuration. Biotechnol Prog 7:237–245.

Flynn DM, Nijjar S, Hubscher SG, de Goyet Jde V, Kelly DA, Strain AJ, Crosby HA. 2004. The role of Notch receptor expression in bile duct development and disease. J Pathol 204:55–64.

Haouzi D, Baghdiguian S, Granier G, Travo P, Mangeat P, Hibner U. 2005. Three-dimensional polarization sensitizes hepatocytes to Fas/CD95 apoptotic signalling. J Cell Sci 118:2763–2773.

Hebner C, Weaver VM, Debnath J. 2008. Modeling morphogenesis and oncogenesis in three-dimensional breast epithelial cultures. Annu Rev Pathol 3:313–339.

Joraku A, Sullivan CA, Yoo J, Atala A. 2007. In-vitro reconstitution of three-dimensional human salivary gland tissue structures. Differentiation 75:318–324.

Kleinman HK, Martin GR. 2005. Matrigel: Basement membrane matrix with biological activity. Semin Cancer Biol 15:378–386.

Kono Y, Yang S, Letarte M, Roberts EA. 1995. Establishment of a human hepatocyte line derived from primary culture in a collagen gel sandwich culture system. Exp Cell Res 221:478–485.

Labarca C, Paigen K. 1980. A simple rapid, and sensitive DNA assay procedure. Anal Biochem 102:344–352.

Landry J, Bernier D, Ouellet C, Goyette R, Marceau N. 1985. Spheroidal aggregate culture of rat liver cells: Histotypic reorganization, biomatrix deposition, and maintenance of functional activities. J Cell Biol 101:914–923.

LeCluyse E, Bullock P, Parkinson A. 1996. Strategies for restoration and maintenance of normal hepatic structure and function in long-term cultures of rat hepatocytes. Adv Drug Del Rev 22:133–186.

Lin HH, Yang TP, Jiang ST, Yang HY, Tang MJ. 1999. Bcl-2 overexpression prevents apoptosis-induced Madin-Darby canine kidney simple epithelial cyst formation. Kidney Int 55:168–178.

Moghe PV, Berthiaume F, Ezzell RM, Toner M, Tompkins RG, Yarmush ML. 1996. Culture matrix configuration and composition in the maintenance of hepatocyte polarity and function. Biomaterials 17:373–385.

Moll R, Franke WW, Schiller DL, Geiger B, Krepler R. 1982. The catalog of human cytokeratins: Patterns of expression in normal epithelia, tumors and cultured cells. Cell 31:11–24.

Nelson CM, Bissell MJ. 2006. Of extracellular matrix, scaffolds, and signaling: Tissue architecture regulates development, homeostasis, and cancer. Annu Rev Cell Dev Biol 22:287–309.

Ng S, Han R, Chang S, Ni J, Hunziker W, Goryachev AB, Ong SH, Yu H. 2006. Improved hepatocyte excretory function by immediate presentation of polarity cues. Tissue Eng 12:2181–2191.

Nishikawa Y, Doi Y, Watanabe H, Tokairin T, Omori Y, Su M, Yoshioka T, Enomoto K. 2005. Transdifferentiation of mature rat hepatocytes into bile duct-like cells in vitro. Am J Pathol 166:1077–1088.

O'Brien LE, Zegers MM, Mostov KE. 2002. Opinion: Building epithelial architecture: Insights from three-dimensional culture models. Nat Rev Mol Cell Biol 3:531–537.

Pollack AL, Runyan RB, Mostov KE. 1998. Morphogenetic mechanisms of epithelial tubulogenesis: MDCK cell polarity is transiently rearranged without loss of cell-cell contact during scatter factor/hepatocyte growth factor-induced tubulogenesis. Dev Biol 204:64–79.

Richert L, Binda D, Hamilton G, Viollon-Abadie C, Alexandre E, Bigot-Lasserre D, Bars R, Coassolo P, LeCluyse E. 2002. Evaluation of the effect of culture configuration on morphology, survival time, antioxidant status and metabolic capacities of cultured rat hepatocytes. Toxicol In Vitro 16: 89–99.

Rotman B, Papermaster BW. 1966. Membrane properties of living mammalian cells as studied by enzymatic hydrolysis of fluorogenic esters. Proc Natl Acad Sci USA 55:134–141.

Sasse D, Spornitz UM, Maly IP. 1992. Liver architecture. Enzyme 46:8–32.

Scholzen T, Gerdes J. 2000. The Ki-67 protein: From the known and the unknown. J Cell Physiol 182:311–322.

Schug M, Heise T, Bauer A, Storm D, Blaszkewicz M, Bedawy E, Brulport M, Geppert B, Hermes M, Follmann W, Rapp K, Maccoux L, Schormann W, Appel KE, Oberemm A, Gundert-Remy U, Hengstler JG. 2008. Primary rat hepatocytes as in vitro system for gene expression studies: Comparison of sandwich, Matrigel and 2D cultures. Arch Toxicol 82:923–931.

Shanks MR, Cassio D, Lecoq O, Hubbard AL. 1994. An improved polarized rat hepatoma hybrid cell line. Generation and comparison with its hepatoma relatives and hepatocytes in vivo. J Cell Sci 107(Pt 4):813–825.

Simon-Assmann P, Leberquier C, Molto N, Uezato T, Bouziges F, Kedinger M. 1994. Adhesive properties and integrin expression profiles of two colonic cancer populations differing by their spreading on laminin. J Cell Sci 107(Pt 3):577–587.

Stamatoglou SC, Hughes RC. 1994. Cell adhesion molecules in liver function and pattern formation. FASEB J 8:420–427.

Szlavik V, Vag J, Marko K, Demeter K, Madarasz E, Olah I, Zelles T, O'Connell BC, Varga G. 2008. Matrigel-induced acinar differentiation is followed by apoptosis in HSG cells. J Cell Biochem 103:284–295.

Tanimizu N, Miyajima A. 2004. Notch signaling controls hepatoblast differentiation by altering the expression of liver-enriched transcription factors. J Cell Sci 117:3165–3174.

Tanimizu N, Miyajima A, Mostov KE. 2007. Liver progenitor cells develop cholangiocyte-type epithelial polarity in three-dimensional culture. Mol Biol Cell 18:1472–1479.

Toda S, Sugihara H. 1990. Reconstruction of thyroid follicles from isolated porcine follicle cells in three-dimensional collagen gel culture. Endocrinology 126:2027–2034.

Wang W, Soroka CJ, Mennone A, Rahner C, Harry K, Pypaert M, Boyer JL. 2006. Radixin is required to maintain apical canalicular membrane structure and function in rat hepatocytes. Gastroenterology 131:878–884.

Xu R, Nelson CM, Muschler JL, Veiseh M, Vonderhaar BK, Bissell MJ. 2009. Sustained activation of STAT5 is essential for chromatin remodeling and maintenance of mammary-specific function. J Cell Biol 184: 57–66.

Yap AS, Stevenson BR, Armstrong JW, Keast JR, Manley SW. 1994. Thyroid epithelial morphogenesis in vitro: A role for bumetanide-sensitive Cl^- secretion during follicular lumen development. Exp Cell Res 213:319–326.

Zhu D. 1979. Establishment and comparison of non-malignant liver cell QSG-7701 and liver cancer cells. [Article in Chinese]. Res Cancer Prev Treat 5:7–9.

Zong Y, Panikkar A, Xu J, Antoniou A, Raynaud P, Lemaigre F, Stanger BZ. 2009. Notch signaling controls liver development by regulating biliary differentiation. Development 136:1727–39.